Electronic Supporting Information for:

Mechanically and chemically robust ZIF-8 monoliths with high volumetric adsorption capacity

Tian Tian,[a] Jose Velazquez-Garcia,[a] Thomas D. Bennett[b] and David Fairen-Jimenez[a,*]

[a]*Department of Chemical Engineering & Biotechnology, University of Cambridge, Pembroke Street, Cambridge CB2 3RA, United Kingdom. Email: df334@cam.ac.uk; website: http://people.ds.cam.ac.uk/df334*

[b]*Department of Materials Science and Metallurgy, University of Cambridge, 27 Charles Babbage Road, Cambridge CB3 0FS, United Kingdom*

Contents

S1 Transmission Electron Microscopy (TEM)

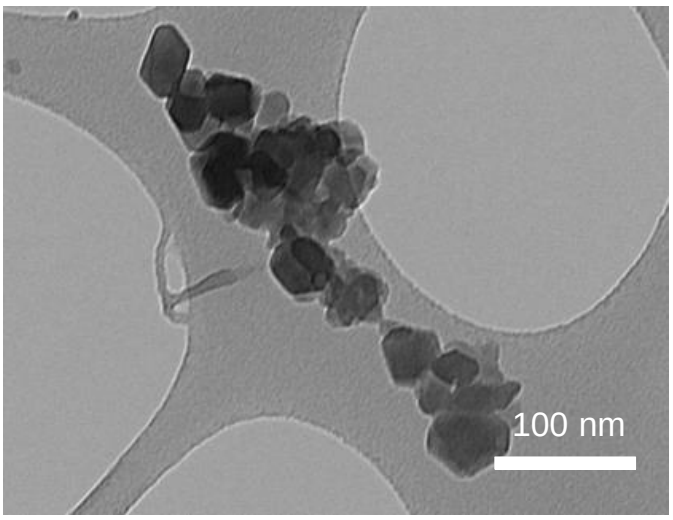

Fig. S1 TEM image of ZIF-8.

S2 X-ray Powder Diffraction

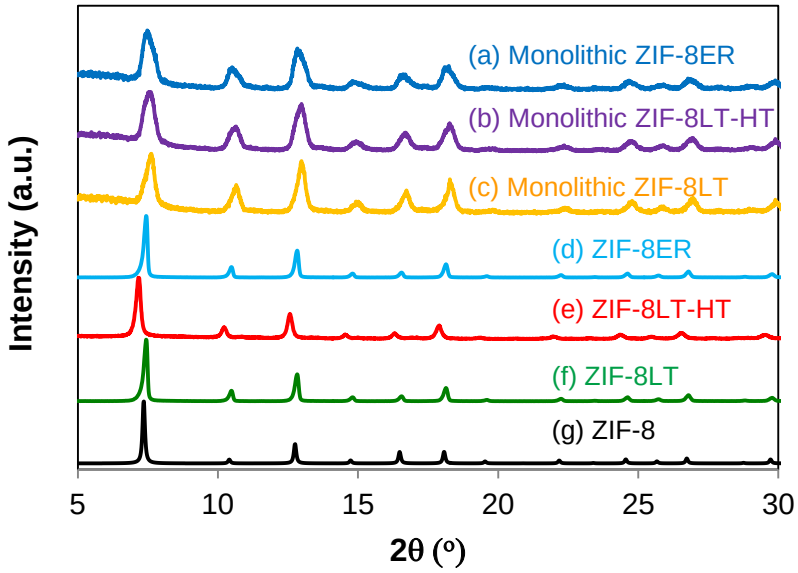

Fig. S2 X-ray diffraction patterns of ZIF-8 monoliths before grinding (a-c) and after grinding (d-f) compared with the simulated pattern (g). Note that the position of the peaks and relative intensities from monolithic and grinded samples are similar.

S3 N_2 adsorption isotherm

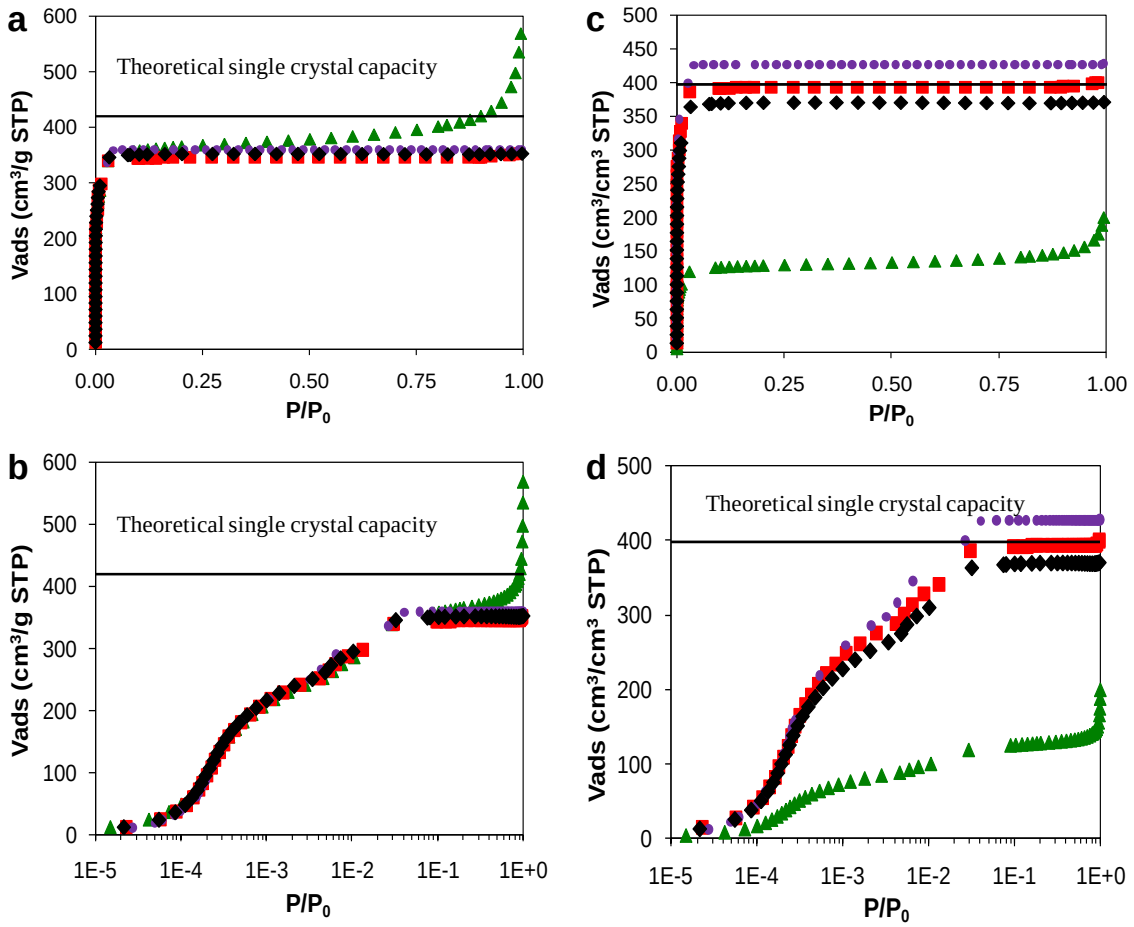

Fig. S3 N_2 Adsorption isotherms at 77 K for ZIF-8LT, red squares, ZIF-8HT, green triangles, ZIF-8LT-HT, black diamonds, and ZIF-8ER, purple circles, in a semi-logarithmic (*left*) and linear (*right*) scale.

Table S1 Gravimetric and volumetric BET areas (S_{BET}), micropore volume (W_0), meso- and macropore volume (V_2), total pore volume (V_{Tot}) and bulk density (ρ_b) for the different ZIF-8 structures.

Material	S_{BET}	W_0[a]	V_2	V_{Tot}[b]	ρ_b[c]	S_{BET}(vol)	W_0(vol)	V_2(vol)	V_{Tot}(vol)
	m^2/g	cm^3/g	cm^3/g	cm^3/g	g/cm^3	m^2/cm^3	cm^3/cm^3	cm^3/cm^3	cm^3/cm^3
ZIF-8HT	1387	0.552	0.277	0.829	0.35[d]	403	0.193	0.097	0.29
ZIF-8LT	1359	0.532	0.011	0.543	1.14	1594	0.606	0.013	0.619
ZIF-8LT-HT	1423	0.543	0.003	0.546	1.05	1494	0.570	0.003	0.573
ZIF-8ER	1395	0.535	0.010	0.545	1.19	1660	0.637	0.012	0.648

S4 Mercury porosimetry

Based on Archimedes' method, it allows measuring the total volume including the volume of the skeleton and the porosity of the MOF samples since mercury at ambient pressure does not penetrate any micro-, meso- and macroporosity. Bulk densities of the samples can be calculated by dividing the mass of the sample by the total volume. Figure S20 shows the pore size distribution of the macro- and mesoporosity of the samples.

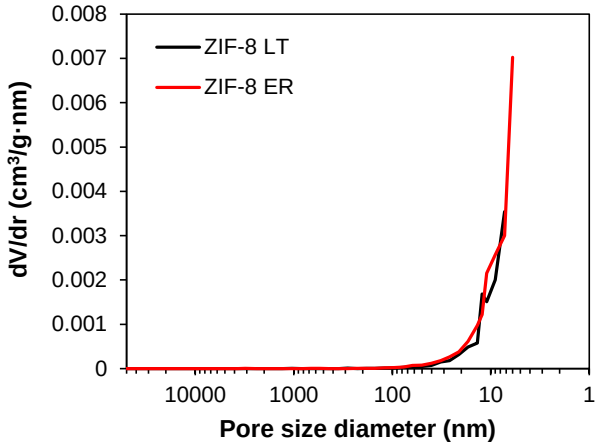

Fig. S4 Pore size distribution of the macro- and mesoporosity of ZIF-8LT and ZIF-8ER

S5 Nanoindentation

ZIF-8LT:

45 indents of 1000nm were performed (10 below on graph)

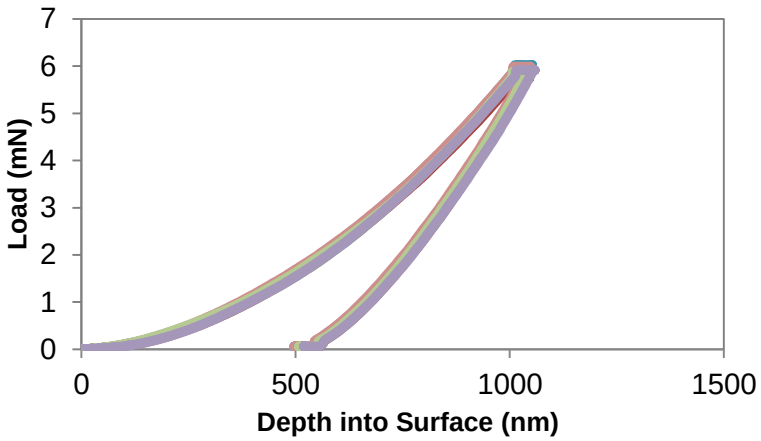

Fig. S5 Load-displacement data for 20 indents on ZIF-8LT, showing excellent consistency.

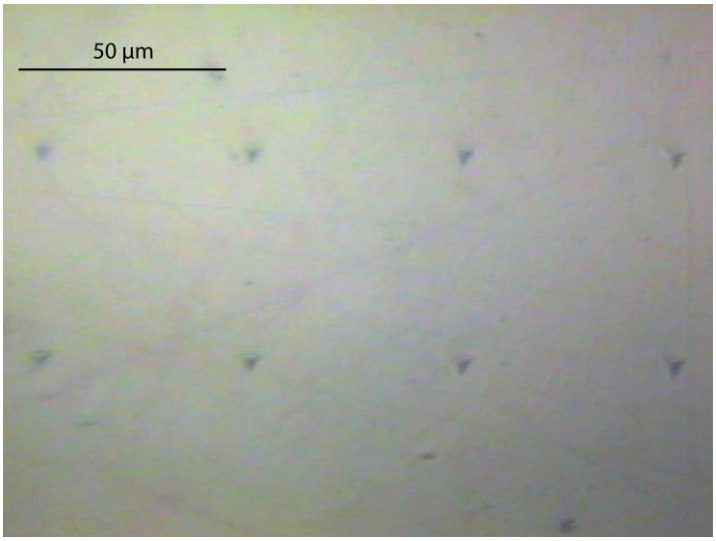

Fig. S6 2 Rows of 1000 nm indents made on a sample (5 x 5 mm) of ZIF-8LT.

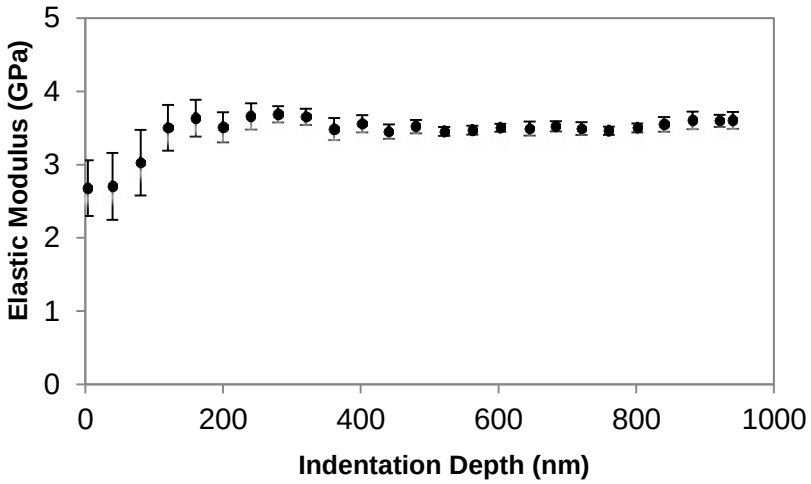

Fig. S7 Elastic moduli of ZIF-8LT as a function of indentation depth, each error bar arises from the standard deviation of 45 indents.

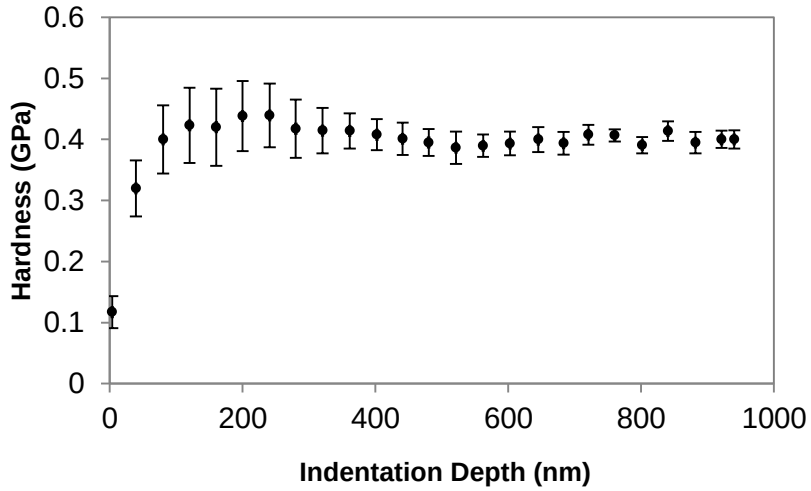

Fig. S8 Hardness of ZIF-8LT as a function of indentation depth, each error bar arises from the standard deviation of 45 indents.

ZIF-8LT-HT:

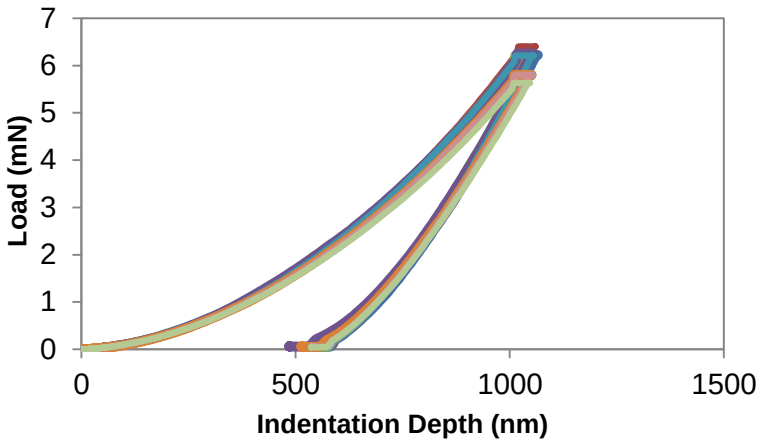

Fig. S9 Load-displacement data for 20 indents on ZIF-8LT-HT.

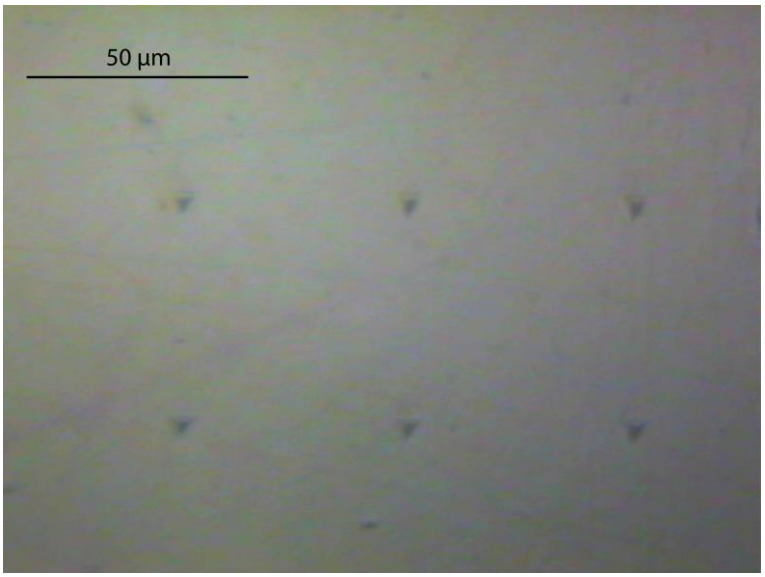

Fig. S10 2 Rows of 1000 nm indents made on a sample (5 x 5 mm) of ZIF-8LT-HT.

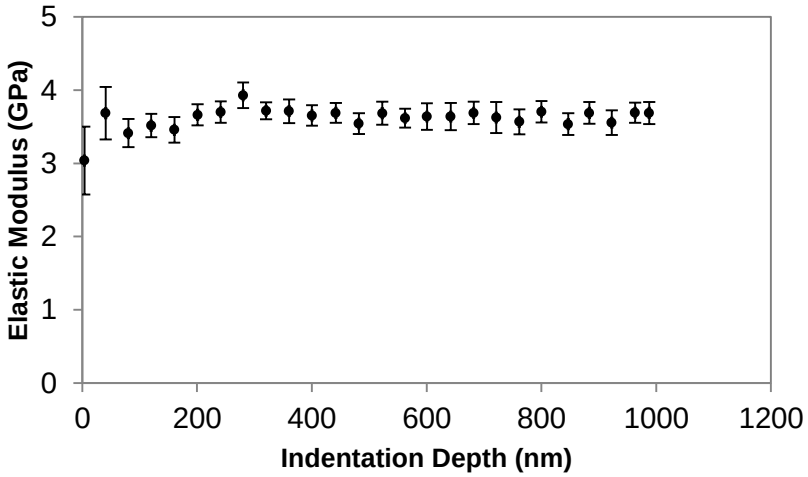

Fig. S11 Elastic moduli of ZIF-8LT-HT as a function of indentation depth, each error bar arises from the standard deviation of 45 indents.

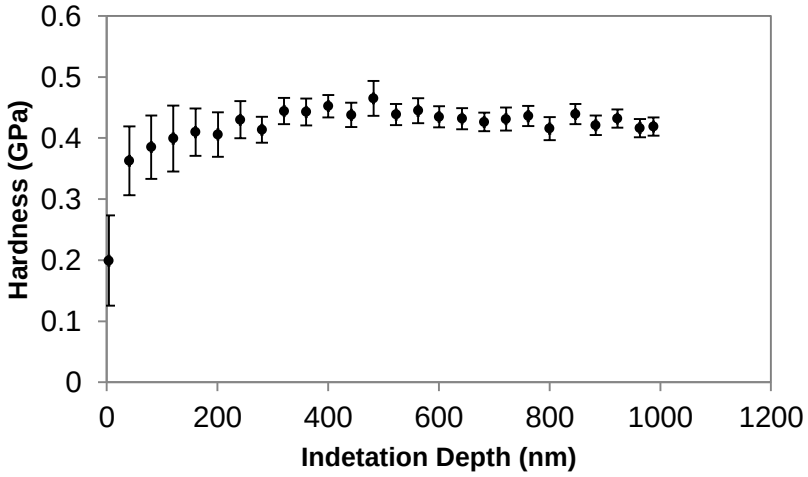

Fig. S12 Hardness of ZIF-8LT-HT as a function of indentation depth, each error bar arises from the standard deviation of 45 indents.

ZIF-8ER

A) 15 indents of 1000 nm depth performed on one monolith

B) 6 indents of 3000 nm performed on a second monolith.

A) 3000nm data set:

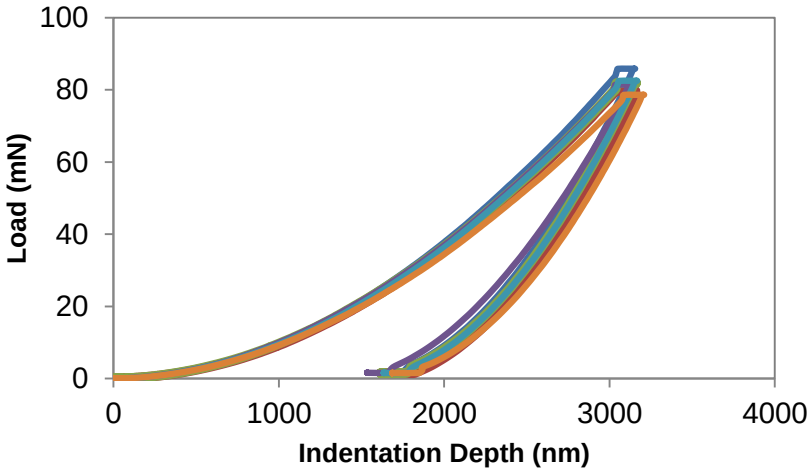

Fig. S13 Load-displacement data for 6 indents on ZIF-8ER.

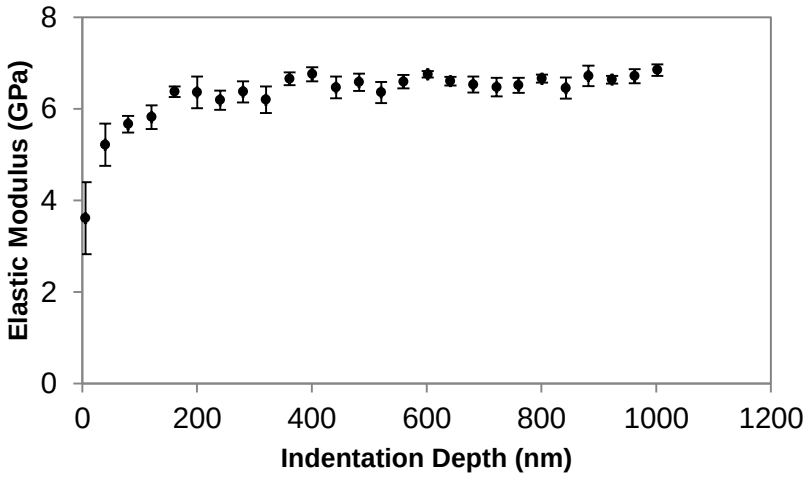

Fig. S14 Elastic moduli of ZIF-8ER as a function of indentation depth, each error bar arises from the standard deviation of 6 indents.

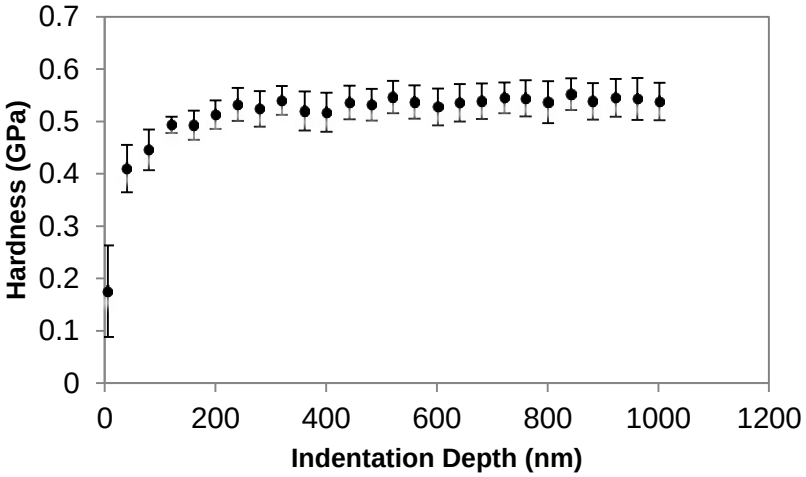

Fig. S15 Hardness of ZIF-8ER as a function of indentation depth, each error bar arises from the standard deviation of 6 indents.

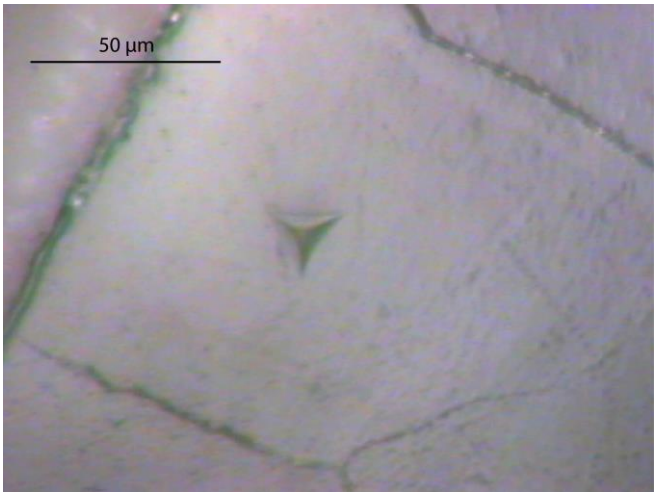

Fig. S16 1000 nm indent made on a sample (5 x 5 mm) of ZIF-8ER.

B) 1000 nm data set:

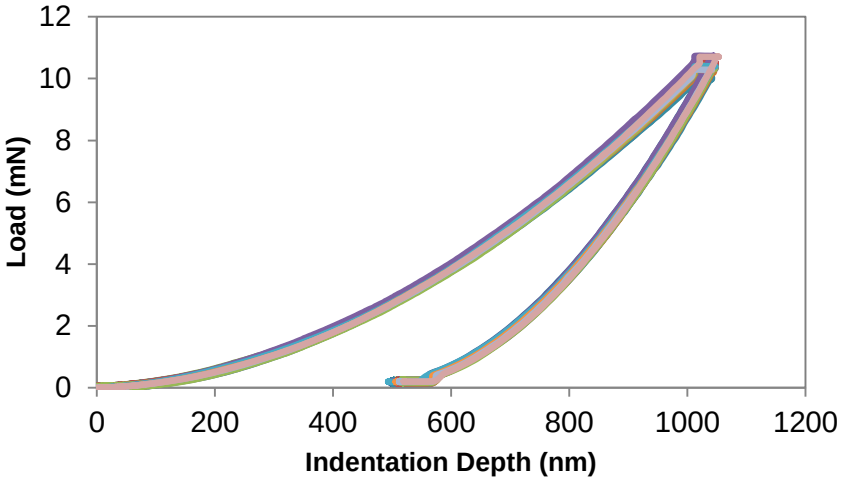

Fig. S17 Load-displacement data for 15 indents on ZIF-8ER.

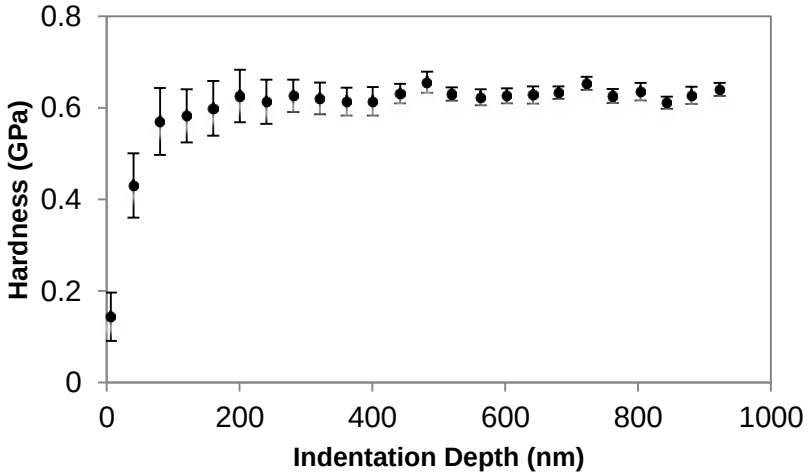

Fig. S18 Hardness of ZIF-8ER as a function of indentation depth, each error bar arises from the standard deviation of 15 indents.

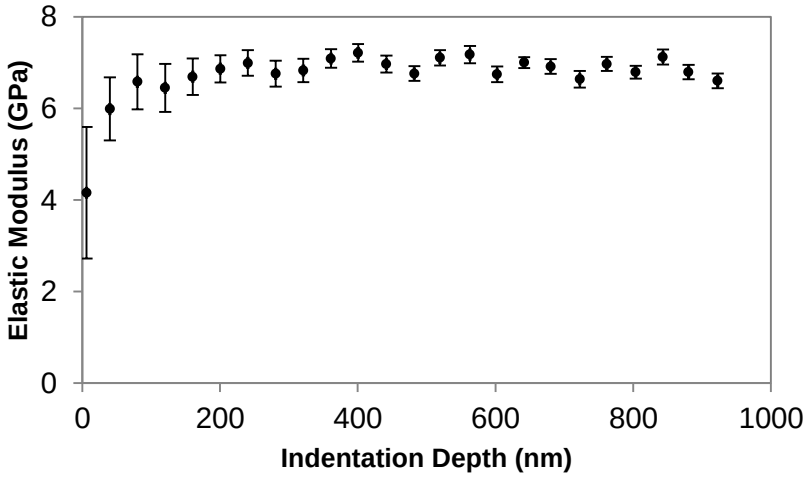

Fig. S19 Elastic moduli of ZIF-8ER as a function of indentation depth, each error bar arises from the standard deviation of 15 indents.

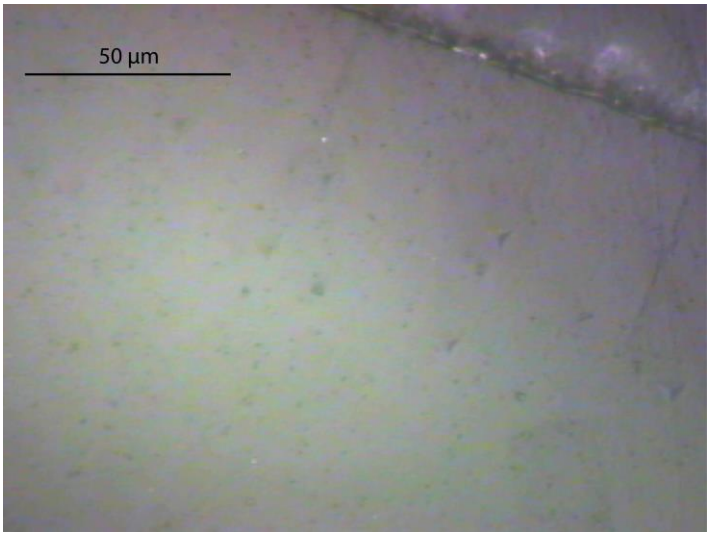

Fig. S20 2 Rows of 1000 nm indents made on a sample (5 x 5 mm) of ZIF-8ER.

S6 Chemical stability

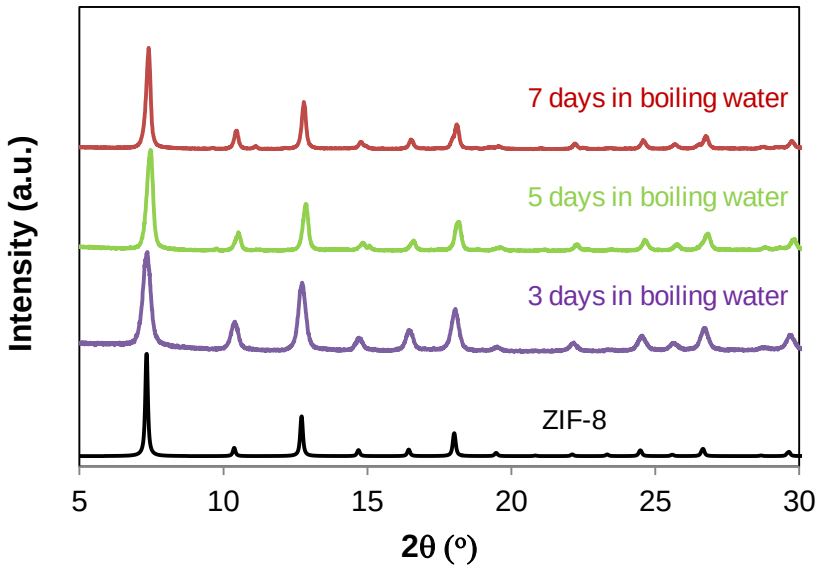

Fig. S21 PXRD patterns of ZIF-8-ER immersed in boiling water alongside a simulated pattern of ZIF-8.